

Yuri Izyumov  
Ernst Kurmaev

SPRINGER SERIES IN MATERIALS SCIENCE 143

# High- $T_c$ Superconductors Based on FeAs Compounds

 Springer



Springer Series in  
**MATERIALS SCIENCE**

---

*Editors:* R. Hull C. Jagadish R.M. Osgood, Jr. J. Parisi Z. Wang H. Warlimont

The Springer Series in Materials Science covers the complete spectrum of materials physics, including fundamental principles, physical properties, materials theory and design. Recognizing the increasing importance of materials science in future device technologies, the book titles in this series reflect the state-of-the-art in understanding and controlling the structure and properties of all important classes of materials.

Please view available titles in *Springer Series in Materials Science*  
on series homepage <http://www.springer.com/series/856>

Yuri Izyumov  
Ernst Kurmaev

# High- $T_c$ Superconductors Based on FeAs Compounds

With 180 Figures

 Springer

Professor Yuri Izyumov  
Ernst Kurmaev  
Russian Academy of Sciences  
Institute of Metal Physics  
S. Kovalevskoy St. 18, 620990 Ekaterinburg, GSP-170, Russia  
E-mail: yuri.izyumov@uran.ru, kurmaev@ifmlrs.uran.ru

*Series Editors:*

Professor Robert Hull  
University of Virginia  
Dept. of Materials Science and Engineering  
Thornton Hall  
Charlottesville, VA 22903-2442, USA

Professor Jürgen Parisi  
Universität Oldenburg, Fachbereich Physik  
Abt. Energie- und Halbleiterforschung  
Carl-von-Ossietzky-Straße 9-11  
26129 Oldenburg, Germany

Professor Chennupati Jagadish  
Australian National University  
Research School of Physics and Engineering  
J4-22, Carver Building  
Canberra ACT 0200, Australia

Dr. Zhiming Wang  
University of Arkansas  
Department of Physics  
835 W. Dickson St.  
Fayetteville, AR 72701, USA

Professor R. M. Osgood, Jr.  
Microelectronics Science Laboratory  
Department of Electrical Engineering  
Columbia University  
Seeley W. Mudd Building  
New York, NY 10027, USA

Professor Hans Warlimont  
DSL Dresden Material-Innovation GmbH  
Pirnaer Landstr. 176  
01257 Dresden, Germany

Springer Series in Materials Science ISSN 0933-033X  
ISBN 978-3-642-14529-2 e-ISBN 978-3-642-14530-8  
DOI 10.1007/978-3-642-14530-8  
Springer Heidelberg Dordrecht London New York

© Springer-Verlag Berlin Heidelberg 2010

This work is subject to copyright. All rights are reserved, whether the whole or part of the material is concerned, specifically the rights of translation, reprinting, reuse of illustrations, recitation, broadcasting, reproduction on microfilm or in any other way, and storage in data banks. Duplication of this publication or parts thereof is permitted only under the provisions of the German Copyright Law of September 9, 1965, in its current version, and permission for use must always be obtained from Springer. Violations are liable to prosecution under the German Copyright Law.

The use of general descriptive names, registered names, trademarks, etc. in this publication does not imply, even in the absence of a specific statement, that such names are exempt from the relevant protective laws and regulations and therefore free for general use.

*Cover design:* eStudio Calamar Steinen

Printed on acid-free paper

Springer is part of Springer Science+Business Media (www.springer.com)

# Preface

In the course of a year or slightly more that passed since the discovery of a new class of high-temperature superconductors (HTSCs) in FeAs-based compounds [1], the world's community of physicists, chemists and technologists achieved a substantial progress in understanding the mechanisms and details of this superconductivity. The intensity of researches coming about is comparable only to that which accompanied the discovery of HTSCs in cuprates. However, the present scientific context is markedly different from that having existed twenty years back. In those times, the researchers moved on while blindly palpating the terrain. At present, they can rely on a rich accumulated experience of work with complex compounds; novel experimental methods and numerical calculation schemes have emerged; computational resources became by far much more powerful, and, last but not least, the physical ideas elaborated in the studies of cuprates could have been immediately adapted for the study of new HTSC compounds.

An unprecedentedly fast advance of researches on the FeAs compounds was helped by an instantaneous propagation of knowledge via electronic data archives. A markedly international character of studies is noteworthy; as a rule, the articles on FeAs systems are published by joint teams of distant lands and laboratories that boosts a rapid augmentation of knowledge about the properties of systems under study and thinking over the wealth of experimental data. During last years (2008–2010), more than few thousand publications within this domain have appeared. This means that every day brought about, on an average, 2–3 new papers deposited in electronic archives.

If the epic of HTSC study in cuprates demanded years for arriving at some understanding of these materials' nature, with respect to new class of materials one year was sufficient as a due time to make a primary overview of the results obtained. Within half a year after the discovery of HTSC in FeAs compounds, first three reviews appeared in the *Physics – Uspekhi* [2–4]. In the beginning of 2009, a special issues of *Physica C* [5] and *New Journal of Physics* [6] appeared with review articles by leading scientists on the basics of the physics of the FeAs compounds, which also summarized the bulk of results accumulated within a year.

This book seems to be the world's first monograph on the physics of FeAs systems. It outlines in a systematic way the results of researches done in the global scientific community throughout the whole period since the end of February

2008, as the high-temperature superconductivity has been discovered in a LaOFeAs system.

The first three chapters cover experimental investigations of all classes of the FeAs compounds in which superconducting state has been discovered. The fourth chapter is devoted to theory models of these compounds and to the discussion, on this basis, of experimental results. Differently from the reviews published in [5, 6], which specifically addressed various aspects of the physics of FeAs systems in some detail, we attempted here to cover, within a unique concept, the whole bulk of experimental and theoretical material on these systems by now available. The authors' hope is that the book be of use for a broad fold of readers: those who already immediately work in this problem and who would wish to enter it.

Russia  
August 2010

*Yu. A. Izyumov*  
*E.Z. Kurmaev*

# Contents

<b>1</b>	<b>Introduction</b> .....	1
<b>2</b>	<b>Compounds of the ReOFeAs Type</b> .....	5
2.1	Crystallochemistry and Basic Physical Properties of Doped Compounds .....	5
2.1.1	Crystal Structure .....	5
2.1.2	Electron Doping .....	5
2.1.3	Hole Doping .....	8
2.1.4	Substitutions on the Fe Sublattice.....	9
2.1.5	Superconducting Transition Temperature .....	11
2.1.6	Critical Fields .....	13
2.1.7	Effect of Pressure on the $T_c$ .....	14
2.2	Magnetic Properties.....	18
2.2.1	Magnetic Structure.....	18
2.2.2	Theoretical Explanation of Long-Range Magnetic Ordering in ReOFeAs.....	20
2.2.3	Phase Diagrams .....	24
2.2.4	Magnetic Fluctuations .....	27
2.3	Electronic Structure .....	28
2.3.1	Stoichiometric Compounds .....	28
2.3.2	The Role of Magnetic Ordering and Doping .....	34
2.3.3	Experimental Studies of the Fermi Surface.....	38
2.4	Symmetry of the Superconducting Order Parameter .....	41
2.4.1	Experimental Methods of Determining the Order Parameter .....	41
2.4.2	Nuclear Magnetic Resonance .....	42
2.4.3	Point-Contact Andreev Reflection .....	46
2.4.4	Tunnel and Photoemission Spectroscopies (STS, PES, ARPES) .....	53
<b>3</b>	<b>Compounds of the AFe<sub>2</sub>As<sub>2</sub> (A = Ba,Sr,Ca) Type</b> .....	57
3.1	Crystal and Electronic Structure.....	57
3.1.1	Crystal Structure .....	57
3.1.2	LDA Calculations of the Electronic Structure.....	58

3.1.3	Experimental Studies of the Fermi Surface.....	63
3.1.4	( $\text{Sr}_3\text{Sc}_2\text{O}_5$ ) $\text{Fe}_2\text{As}_2$ and Other Similar Compounds .....	69
3.2	Superconductivity .....	72
3.2.1	Doping .....	72
3.2.2	Coexistence of Superconductivity and Magnetism.....	77
3.2.3	Effect of Pressure .....	79
3.2.4	Symmetry of the Superconducting Order Parameter.....	88
3.2.5	Measurements on the Josephson Contacts.....	94
3.2.6	Critical Fields .....	96
3.3	Magnetism.....	98
3.3.1	Stoichiometric Compounds .....	98
3.3.2	Doped Compounds .....	102
3.3.3	Magnetic Excitations .....	104
<b>4</b>	<b>Other FeAs-Based Compounds.....</b>	<b>109</b>
4.1	Compounds of the FeSe, FeTe Type .....	109
4.1.1	Superconducting Properties .....	109
4.1.2	Unusual Magnetic Properties.....	112
4.1.3	Electronic Structure of Stoichiometric Compounds.....	115
4.1.4	Electronic Structure of Doped Compounds .....	118
4.1.5	Magnetic Structure of FeTe .....	120
4.2	Compounds of the LiFeAs Type .....	122
4.2.1	Superconductivity.....	122
4.2.2	Electronic Structure.....	123
4.3	Compounds of the AFeAs (A = Sr, Ca) Type .....	126
4.3.1	Primary Experimental Observations .....	126
4.3.2	Electronic Structure.....	128
<b>5</b>	<b>Theory Models .....</b>	<b>131</b>
5.1	General Properties of Compounds from Different Classes of FeAs-Systems and Corresponding Theory Objectives .....	131
5.1.1	Crystal and Magnetic Structures .....	131
5.1.2	Peculiarities of the Electronic Structure .....	134
5.1.3	Asymmetry of the Electron/Hole Doping .....	136
5.1.4	Problems of Symmetry of the Superconducting Order Parameter .....	138
5.1.5	Isotopic Effect .....	140
5.2	Role of Electron Correlations .....	141
5.2.1	Dynamical Mean Field Theory (DMFT) .....	141
5.2.2	LDA+DMFT Calculation for ReOFeAs Compounds .....	145
5.2.3	LDA+DMFT Calculation on an Extended Basis .....	148
5.2.4	Comparison with Experiment .....	152
5.3	A Minimal Two-Orbital Model.....	158
5.3.1	Formulation of the Model .....	158
5.3.2	Band Structure of the Spectrum .....	162

- 5.3.3 Mean Field Approximation.....164
- 5.3.4 Numerical Calculation for Small Clusters .....167
- 5.4 Multi-Orbital Model .....170
  - 5.4.1 Formulation of the Model .....170
  - 5.4.2 Equations for a Superconductor in the Fluctuation Exchange (FLEX) Approximation .....171
  - 5.4.3 Properties of Superconductors with the  $s^\pm$  Symmetry of the Order Parameter .....174
  - 5.4.4 Three-Orbital Model.....178
- 5.5 Detailed Analysis of the 5-Orbital Model.....182
  - 5.5.1 The Hamiltonian of the Model .....182
  - 5.5.2 Spin and Charge Susceptibility .....184
  - 5.5.3 Pairing of Electrons via Spin Fluctuations .....187
  - 5.5.4 Possible Symmetries of the Superconducting Order Parameter .....190
- 5.6 Limit of Weak Coulomb Interaction .....194
  - 5.6.1 Renormalization Group Analysis .....194
  - 5.6.2 Equations for Superconducting and Magnetic Order Parameters .....202
  - 5.6.3 Phase Diagram of the Model .....205
  - 5.6.4 Peculiarities of the  $s^\pm$ -Superconducting State .....207
- 5.7 The Limit of Strong Coulomb Interaction .....210
  - 5.7.1 The  $t - J_1 - J_2$ -Model .....210
  - 5.7.2 Superconductivity with Different Order Parameters .....212
  - 5.7.3 Density of States and Differential Tunnel Conductivity .....215
  - 5.7.4 The Hubbard Model with the Hund’s Exchange .....217
- 5.8 Magnetic Long-Range Order and Its Fluctuations .....221
  - 5.8.1 Two Approaches to the Problem .....221
  - 5.8.2 The Itinerant Model.....224
  - 5.8.3 The Localized Model: Spin Waves.....228
  - 5.8.4 The Resonance Mode.....233
  - 5.8.5 Unified Models .....240
  - 5.8.6 FeAs-Compounds as Systems with Moderate Electron Correlations .....245
- 5.9 Orbital Ordering.....247
  - 5.9.1 The Spin-Orbital Model .....247
  - 5.9.2 Phase Diagrams with Spin and Orbital Orderings.....250
  - 5.9.3 Spectrum of Magnetic Excitations .....251
- Conclusion** .....255
- References**.....259
- Index**.....277



# Acronyms

1111	compounds of type LaOFeAs
122	compounds of type BaFe <sub>2</sub> As <sub>2</sub>
111	compounds of type LiFeAs
11	compounds of type FeSe
<i>LDA</i>	Local Density Approximation
<i>LSDA</i>	Local Spin Density Approximation
<i>DMFT</i>	Dynamical Mean Field Theory
<i>LDA + DMFT</i>	joint <i>LDA</i> and <i>DMFT</i> computational scheme
<i>RPA</i>	Random-Phase Approximation
<i>FLEX</i>	Fluctuation Exchange Interaction
<i>Folded BZ</i>	Folded BZ
<i>Unfolded BZ</i>	Unfolded BZ
<i>SDW</i>	Spin Density Wave
<i>CDW</i>	Charge Density Wave
<i>NMR</i>	Nuclear Magnetic Resonance
<i>STS</i>	Scanning Tunneling Microscopy
<i>PCAR</i>	Point-Contact Andreev Reflection
<i>PES</i>	Photoelectron spectroscopy
<i>ARPES</i>	Angle Resolved Photoelectron Spectroscopy
<i>RXES</i>	Resonant X-Ray Emission Spectroscopy
<i>ZBC</i>	Zero-Bias conductance
<i>HTSC</i>	High Temperature Superconductivity
<i>OP</i>	Order Parameter
<i>GF</i>	Green Function
<i>BCS</i>	Bardin–Cooper–Schrieffer’s theory

# Chapter 1

## Introduction

The first report of superconductivity in LaOFeAs appeared in 2006 [1]; however, the transition temperature was low,  $T_c = 3.5$  K. Similarly, LaONiP have shown  $T_c = 4.5$  K [7]. The breakthrough occurred in February 2008, as Kamihara et al. reported a superconductivity with  $T_c = 26$  K in fluorine-doped compound LaO<sub>1-x</sub>F<sub>x</sub>FeAs [8]. Immediately afterwards several Chinese groups, by substituting lanthanum with other rare-earth elements, achieved much higher  $T_c$  values, namely, 41 K in CeO<sub>1-x</sub>F<sub>x</sub>FeAs [9], 52 K in PrO<sub>1-x</sub>F<sub>x</sub>FeAs [10] and reached 55 K in SmO<sub>1-x</sub>F<sub>x</sub>FeAs [11].

The pristine (undoped) compounds are antiferromagnetic (AFM) metals, in which the magnetic ordering comes about simultaneously with structural phase transition at the Neél temperature  $T_N \approx 140$  K (in LaOFeAs) from tetragonal to orthorhombic phase. On substituting oxygen with fluorine,  $T_N$  rapidly falls down as the F concentration increases, and at  $x \simeq 0.1$  the long-range magnetic ordering disappears, and a superconducting state sets on. A typical phase diagram of this type of compounds is shown in Fig. 1.1 in the  $(T, x)$  plane [12].

The situation so far resembles the HTSC in cuprates, e.g., (La<sub>1-x</sub>Sr<sub>x</sub>)<sub>2</sub>CuO<sub>4</sub> exhibits a similar phase diagram. The superconductivity appears there in compounds of the type La<sub>2</sub>CuO<sub>4</sub>, which are also AFM under stoichiometry, in the course of lanthanum being substituted by strontium. In both systems, the doping brings along charge carriers (electrons or holes) that suppresses the AFM ordering and creates conditions for forming the Cooper pairs. This analogy supported a suggestion that the high- $T_c$  superconductivity in newly discovered FeAs-based systems is influenced by the system's closeness to a magnetic phase transition, so that high  $T_c$  values are due to the carriers pairing mechanism via spin fluctuations.

An analogy between FeAs systems and cuprates becomes more apparent if we compare their crystal structures. The FeAs-based systems are built by stapling of the FeAs planes, intermediated by the LaO layers, similarly to how in cuprates the stacked CuO<sub>2</sub> planes are separated by the La- or Y-Ba layers. By force of their layered structure, both types of systems are strongly anisotropic, and electronic states therein are quasi two-dimensional.

Closely following the *Re*OFeAs compounds (with *Re* being a rare-earth element), the compounds of the type AFe<sub>2</sub>As<sub>2</sub>, (A = Ba, Sr, Ca) emerged, whose peculiarity is that a repeated unit in them contains a doubled FeAs plane, similarly to

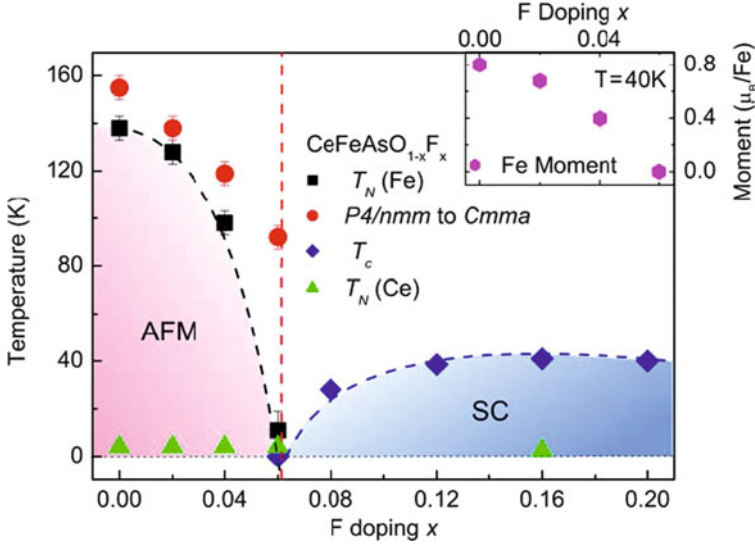


**Fig. 1.1** Phase diagram in the  $(T, x)$  plane for the  $\text{CeO}_{1-x}\text{F}_x\text{FeAs}$  compound

doubled layers in cuprates  $\text{YBa}_2\text{Cu}_3\text{O}_6$ . In doped  $\text{AFe}_2\text{As}_2$ , the superconductivity was immediately found with  $T_c = 38\text{ K}$  [13]. Further on, another class of FeAs-based systems has been discovered, the  $\text{LiFeAs}$  compound in which the FeAs planes are separated by the layers of lithium. It is remarkable that in this compound superconductivity with  $T_c = 18\text{ K}$  appears without any doping [14, 15].

A similar property is revealed by yet another structural type, namely,  $\text{FeSe}$ ,  $\text{FeS}$  and  $\text{FeTe}$ , which are quite resembling the compounds of the FeAs group. These novel compounds are built from iron–chalcogen planes, in which, like in the FeAs compounds, the iron atoms form a squared lattice, each atom being surrounded by an octahedron of chalcogens. Here, no intermediary layers are present. In one such compound,  $\text{FeSe}$ , under pressure of  $\sim 1.5\text{ GPa}$  a superconductive transition with  $T_c = 27\text{ K}$  has been detected [16].

Therefore as of now we are aware of three classes of compounds build of the FeAs layers: these are  $\text{LaOFeAs}$ ,  $\text{AFe}_2\text{As}_2$ ,  $\text{LiFeAs}$  and moreover a similar structure type of  $\text{FeSe}$  in which the superconductivity with high  $T_c$  was detected. Physical properties of these compounds have many similarities and are dominated by the influence of a common planar structural element. More precise analysis of physical properties confirms this suggestion.

Calculations on electron–phonon coupling in these compounds have shown [17, 18] that the standard electron–phonon coupling mechanism cannot account for such high  $T_c$  values.

A similarity in physical properties of the FeAs-compounds with those of high-temperature superconducting cuprates puts forward a question about a role of electron correlations in these new materials. It is known that in the materials on

the basis of transition-metal and rare-earth elements, such correlations do often play a primary role – see, e.g., a monograph by Fulde [19]. Another important question is that concerning the role of degenerate 3d orbitals of the Fe ions in the formation of electronic structure near the Fermi level in the FeAs-compounds, and about the spin state of the Fe ions in the compound [20]. Both these important questions will be addressed in the book from both experimental and theoretical viewpoints.

## Chapter 2

# Compounds of the ReOFeAs Type

### 2.1 Crystallochemistry and Basic Physical Properties of Doped Compounds

#### 2.1.1 Crystal Structure

The highest values of  $T_c$  have been achieved in the row of *Re*OFeAs doped compounds, where *Re* stands for a rare-earth element (Table 2.1). All these compounds possess, at room temperature, a tetragonal structure with the  $P4/nmm$  space group. Their crystal structure is formed by repeated FeAs layers, interlaced by the LaO layers. The FeAs layer is, in fact, created by three closely situated atomic planes: the middle one is a quadratic lattice of Fe atoms, sandwiched between two quadratic lattices of As, so that each atom of iron is surrounded by a tetrahedron of arsenic atoms. In other words, the FeAs layer is, in fact, formed by FeAs<sub>4</sub> complexes. The FeAs and LaO layers are separated by 1.8 Å.

The crystal structure of LaOFeAs is shown in Fig. 2.1. Lattice parameters for the *Re*OFeAs compounds are given in Table 2.1. As is seen, the tetragonal unit cell is strongly elongated, which explains a strong anisotropy of all its properties and a quasi-bidimensional nature of electronic states. The closest to each Fe atom are those of As, which undergo to the next Fe neighbours, so that the electron transfer processes over the Fe sublattice are mediated by the Fe-As hybridization, and the exchange interaction between Fe atoms is of indirect character via the As atoms.

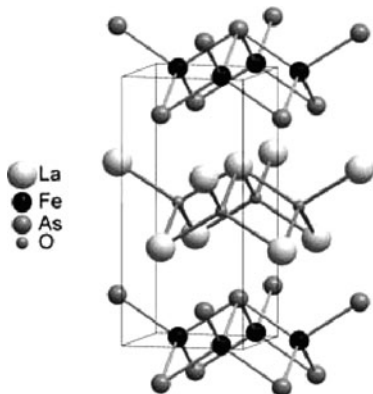
Crystallochemical properties of LaOFeAs compounds are determined by the configuration of the outer electron shells: Fe(4s4p3d), As(4s4p), La(6s5d4f), O(2s2p). The formal valences of ions are as follows: La<sup>3+</sup>O<sup>2-</sup>Fe<sup>2+</sup>As<sup>3-</sup>.

#### 2.1.2 Electron Doping

On substituting an oxygen atom by fluorine, an extra electron goes into the FeAs layer; such situation is commonly referred to as electron doping. A substitution of lanthanum by, say, strontium, the LaO layer would lack one electron, which can be

**Table 2.1** Maximal temperatures of superconducting transitions obtained by doping of the  $ReOFeAs$  compounds. In the last two lines, the lattice parameters of undoped compounds are given

$ReOFeAs$	$La$	$Ce$	$Pr$	$Nd$	$Sm$	$Gd$
$T_c$ , K	41	41	52	51.9	55	53.5
Reference	[27]	[9]	[10]	[28]	[11]	[29]
$a$ , Å	4.035	3.996	3.925	3.940	3.940	
$c$ , Å	8.740	8.648	8.595	8.496	8.496	

**Fig. 2.1** Crystal structure of  $LaOFeAs$ 

borrowed from the  $FeAs$  layer, leaving behind a hole. This would correspond to a hole doping. A re-distribution of electrons between the doped  $LaO$  and  $FeAs$  layers gives rise to a resulting conductivity of a compound. The nature of carriers can be deduced experimentally from the sign of the Hall constant  $R_H$ .

The measurements of the Hall effect have been done on a compound  $LaO_{0.9}F_{0.1}FeAs$  [21] with  $T_c = 24$  K soon after the discovery by Kamihara et al. [8] a superconductivity with  $T_c = 26$  K on this very compound. In [21], it was concluded that  $R_H$  is negative and roughly independent on temperature up to 240 K. This indicates that the conductivity is dominated by electron carriers. From the Hall coefficient measured at  $T \approx 100$  K, the carrier concentration was deduced to be  $9.8 \cdot 10^{20} \text{ cm}^{-3}$ . The authors of [22] confirmed these estimates. A measurement of  $R_H$  on a different sample  $LaO_{0.89}F_{0.11}FeAs$  with  $T_c = 28.2$  K, done at a temperature slightly superior to  $T_c$ , has shown that the concentration of electron carriers  $n \approx 1 \cdot 10^{21} \text{ cm}^{-3}$  [23] does, in fact, coincide with the results of [21, 22] (Fig. 2.2). In the inset of this figure, a temperature behaviour of the Hall coefficient  $R_H$ , throughout negative, is shown.

Another example of electron doping is given in Fig. 2.3 [24], where doped and undoped compounds are compared. In both cases, the Hall coefficient is negative. Compounds with other rare-earth elements, e.g.  $NdO_{0.82}F_{0.18}FeAs$  [25], well indicate an electron nature of carriers.

A remarkable fact was a discovery of high- $T_c$  superconductivity in the compounds  $ReOFeAs$  without fluorine doping, but under oxygen deficiency. Thus, [26]

**Fig. 2.2** Variation of the number of carriers and the Hall coefficient for the  $\text{LaO}_{0.89}\text{F}_{0.11}\text{FeAs}$  compound [23]

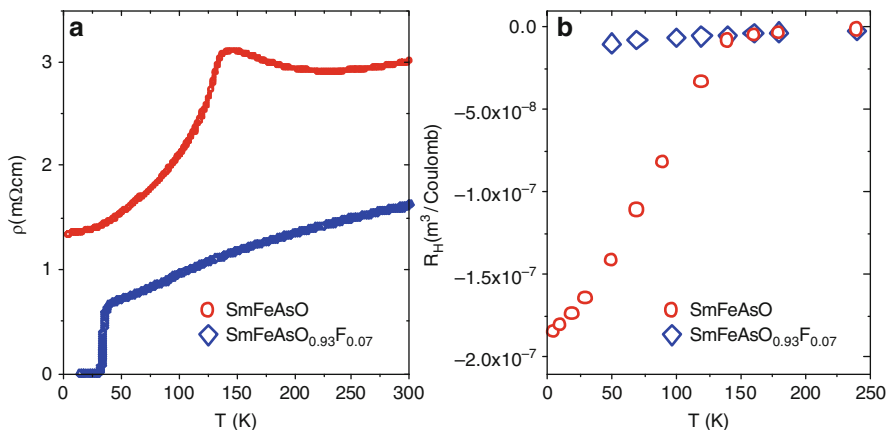
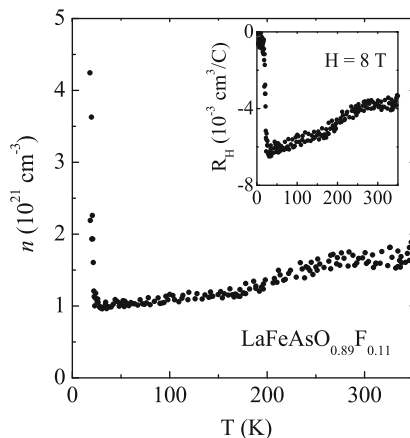


**Fig. 2.3** Temperature dependence of resistivity and Hall coefficient for nondoped  $\text{SmOFeAs}$  and fluorine-doped  $\text{SmO}_{0.93}\text{F}_{0.07}\text{FeAs}$  compound [24]

reports a detection of high  $T_c$  values in  $\text{LaO}_{0.6}\text{FeAs}$  ( $T_c = 28$  K),  $\text{LaO}_{0.75}\text{FeAs}$  ( $T_c = 20$  K), and  $\text{NdO}_{0.6}\text{FeAs}$  ( $T_c = 53$  K).

In [9–11, 27–29], the data are given concerning the compounds  $\text{ReO}_{1-\Delta}\text{FeAs}$  with  $\text{Re} = \text{Sm}, \text{Nd}, \text{Pr}, \text{Ce}, \text{La}$ . Among them, the  $\text{SmO}_{1-\delta}\text{FeAs}$  system indicated the highest  $T_c = 55$  K. Hence, the fluorine doping and the oxygen deficiency produce similar effects in the initial stoichiometric compounds: they create electron carriers, suppress antiferromagnetic (AFM) ordering and result in the formation of a superconducting state.

Let us now consider the effect of substitution of a rare-earth element by a heterovalent dopant. A replacement of trivalent  $\text{Re}^{3+}$  by a tetravalent substituent results in electron doping. For example, we take a system  $\text{Gd}_{1-x}\text{Th}_x\text{OFeAs}$ , where  $\text{Gd}^{3+}$  is substituted by  $\text{Th}^{4+}$ . At  $x \approx 0.1$ , a superconductivity with  $T_c = 55$  K has

been reported by [30]. Another example of electron doping is  $\text{Tb}_{1-x}\text{Th}_x\text{OFeAs}$ , where a substitution of  $\text{Tb}^{3+}$  by  $\text{Th}^{4+}$  results in  $T_c = 52$  K [31].

### 2.1.3 Hole Doping

A completely different situation arises on substituting an  $\text{Re}^{3+}$  ion by a divalent element. On substitution of  $\text{La}^{3+}$  in  $\text{LaOFeAs}$  by  $\text{Sr}^{2+}$ , we deal with hole doping. The resulting compound,  $\text{La}_{1-x}\text{Sr}_x\text{OFeAs}$ , at  $x = 0.13$  becomes superconducting with  $T_c = 25$  K [32]. This was the first superconductor in the FeAs-row, obtained by hole doping, as has been confirmed by measuring the Hall coefficient  $R_H$ , which turned out in this system to be positive [33].

Apparently, an increase in strontium concentration suppresses the conventional AFM ordering in the pristine compound, and already at  $x = 0.03$  the doped state becomes superconducting.  $T_c$  grows along with  $x$  and at  $x \approx 0.11$ – $0.13$  reaches the value of  $T_c = 25$  K. On substituting oxygen by fluorine,  $T_c = 26$  K. We can note a peculiar electron-hole symmetry: on doping a pristine compound by either electrons or holes the  $T_c$  grows in roughly similar way. There is, however, a certain difference between two situations. On doping with Sr, a rise of  $T_c$  is accompanied by a monotonous increase of the lattice parameters  $a$  and  $c$ , whereas fluorine doping reduces the lattice parameters [33].

A system  $\text{Pr}_{1-x}\text{Sr}_x\text{OFeAs}$  offers another example of the hole doping, on substituting  $\text{Pr}^{3+}$  by  $\text{Sr}^{2+}$  [34]. A superconductivity of  $T_c = 16.3$  K was achieved at the Sr concentration  $x \approx 0.20$ – $0.25$ . Figure 2.4 shows a temperature dependence of the Hall coefficient, which is, below the room temperature, throughout positive. A similar result occurs in an Nd-based compound on substitution of the latter element with Sr. In an  $\text{Nd}_{1-x}\text{Sr}_x\text{OFeAs}$  sample ( $0 < x < 0.2$ ),  $T_c = 13.5$  K has been achieved at  $x \approx 0.2$  [35]. It should be noted that in difference from electron-doped compounds such as  $\text{ReO}_{1-x}\text{F}_x\text{FeAs}$  where an increase of  $x$  the magnetic ordering is gradually suppressed and superconductivity occurs already at  $x < 0.1$ , in hole-doped systems

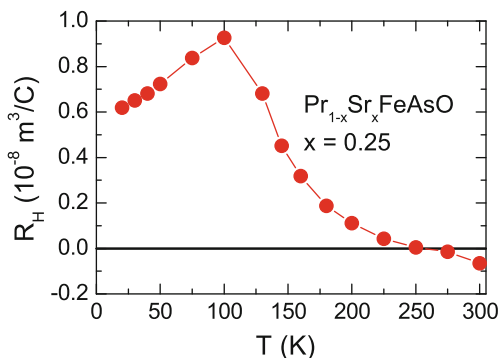


**Fig. 2.4** Temperature dependence of the Hall coefficient  $R_H$  for the hole-doped  $\text{Pr}_{0.75}\text{Sr}_{0.25}\text{OFeAs}$  compound [34]

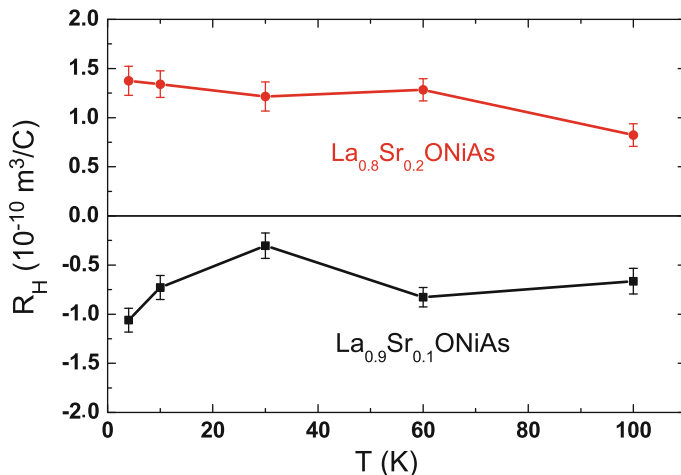


Fig. 2.5 Hall coefficient for two samples of the  $\text{La}_{1-x}\text{Sr}_x\text{ONiAs}$  compound [36]

an onset of a superconducting state demands higher concentrations of dopant. In this sense, the “electron-hole symmetry” does not hold.

The above discussion of main physical properties in  $\text{LaOFeAs}$  systems remains valid for those where Ni takes place of Fe, only that the  $T_c$  in such systems is much lower. It is noteworthy that the nature of carriers – are they holes or electrons – may vary depending on the dopant concentration (Fig. 2.5).

The  $\text{LaOFeAs}$  compound can be doped not only by fluorine which substitutes oxygen, but also by elements taking place of lanthanum, e.g. potassium. A doping with potassium adds hole carriers, rather than electrons. In [37], a new method of synthesis of superconducting compounds on the basis of  $\text{LaOFeAs}$  was suggested, allowing a simultaneous doping with fluorine and potassium. A synthesized compound  $\text{La}_{0.8}\text{K}_{0.2}\text{O}_{0.8}\text{F}_{0.2}\text{FeAs}$  had  $T_c = 28.5 \text{ K}$ .

The examples discussed above show that the superconductivity in  $\text{FeAs}$  systems might be induced either by electron doping (substituting oxygen by fluorine or due to the presence of oxygen vacancies), or by hole doping (via substituting La by Sr). These tendencies are maintained throughout the whole class of the  $\text{ReOFeAs}$  systems.

### 2.1.4 Substitutions on the Fe Sublattice

In earlier stages of studying the  $\text{ReFeAsO}$  system, it was shown that the superconductivity is induced by doping on either oxygen or rare-earth sublattice, which both are beyond the  $\text{FeAs}$  layers. Due to either substitution of oxygen by fluorine, or oxygen deficiency, the  $\text{FeAs}$  layers are infiltrated by charge carriers, that suppresses antiferromagnetic order of the pristine compound and leads to superconductivity.

In this sense, the new superconductors resemble the cuprates, where substitutions occur outside the  $\text{CuO}_2$  planes.

A substitution of Fe atoms in the FeAs layers by Co does as well result in suppression of antiferromagnetism and appearance of superconductivity already at low concentrations of dopant. This feature makes a marked differences of new superconductors from cuprates, in which any intrusion into the  $\text{CuO}_2$  planes suppresses superconductivity. In several works appeared simultaneously, astonishing results have been reported on a number of samples of  $\text{LaOFe}_{1-x}\text{Co}_x\text{As}$  [12, 38, 39]. At  $x = 0.05$ , the antiferromagnetism was suppressed, and at  $x \approx 0.1$  a superconductivity with  $T_c \approx 10$  K emerged, which further on disappeared at  $x > 0.15$ . This is confirmed by temperature dependencies of electrical conductivity at different  $x$  (Fig. 2.6) [38].

The phase diagram of this system in the  $(T, x)$  axes is shown in Fig. 2.7 [39]. It is shown that in the  $x$  range corresponding to superconductivity, for  $T > T_c$  first a semiconductor-type behaviour is observed, which is followed at  $T \approx 100$  K by metallic conductivity. Similar results were obtained for  $\text{SmOFe}_{1-x}\text{Co}_x\text{As}$  [39].

It turns out therefore that Co is an efficient dopant for inducing superconductivity. It is astonishing that superconductivity persists at quite high degree of disorder (broad interval of  $x$ ) that apparently is an argument in favour of a non-standard symmetry of the order parameter, which is not sensitive to magnetic impurities [40]. It is interesting to note that for  $x = 1$  the system becomes ferromagnetic with  $T_c \approx 56$  K [38].

Note that electronic structure calculations for  $\text{LaOFe}_{1-x}\text{Co}_x\text{As}$  have appeared [41], which show that the Co doping displaces the Fermi level from its position at the slope of the partial density of Fe3d states into a more flat region. This circumstance explains a suppression of the SDW transition in the initial LaOFeAs on doping of its Fe sublattice.

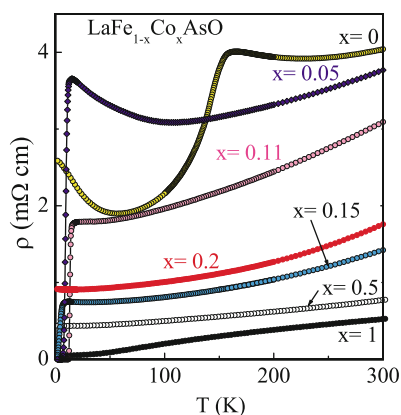


**Fig. 2.6** Temperature dependence of electrical resistivity of the  $\text{LaOFe}_{1-x}\text{Co}_x\text{As}$  compound at different cobalt concentrations [38]

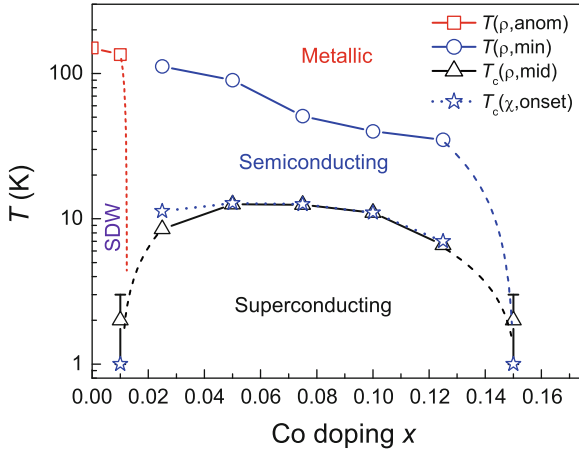


Fig. 2.7 Phase diagram of  $\text{LaOFe}_{1-x}\text{Co}_x\text{As}$  in the  $(T, x)$  plane [39]

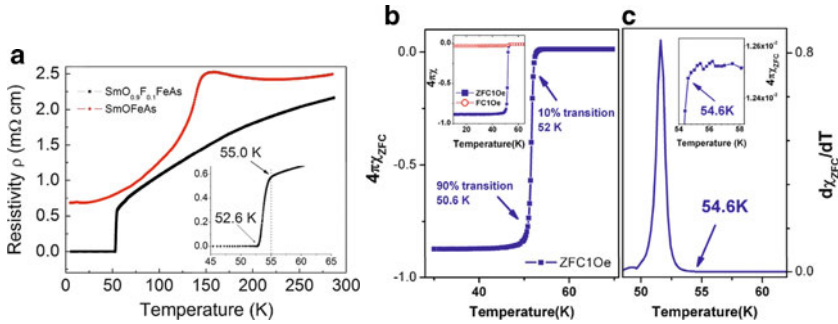
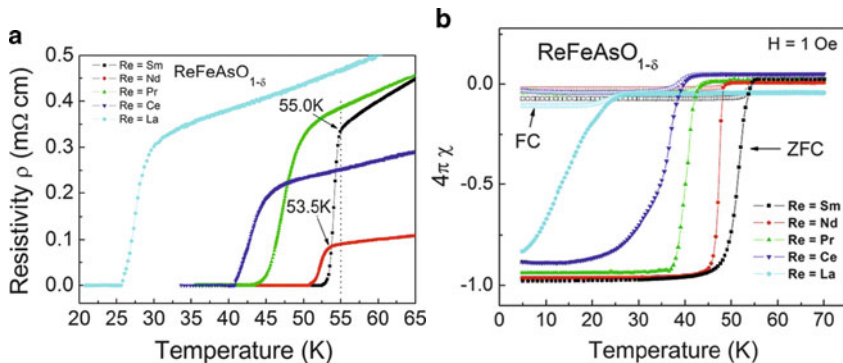


Fig. 2.8 Manifestation of superconducting state in the  $\text{SmO}_{0.9}\text{F}_{0.1}\text{FeAs}$  compound as revealed by temperature dependence of (a) electrical resistivity, (b) magnetic susceptibility  $\chi$ , (c) the derivative of  $\chi$  in temperature [11]

### 2.1.5 Superconducting Transition Temperature

Now we turn to a more detailed description of superconducting properties in FeAs systems. How does a superconducting state in a doped material reveal itself in experiment? Let us take as an example the  $\text{SmO}_{1-x}\text{F}_x\text{FeAs}$  compound in which at  $x = 0.1$  the highest so far value of  $T_c = 55$  K has been obtained [11]. Figure 2.8 shows the results of three different measurements: a sharp drop of electrical conductivity on lowering the temperature, a sharp appearance of diamagnetic response  $\chi$  in applied magnetic field, and a sharp peak in the  $d\chi/dT$  derivative. All three anomalies occur near the same temperature, which is, accordingly, the superconducting transition temperature. The curves as in Fig. 2.8 are typical for all superconducting systems on the FeAs basis. For comparison, corresponding curves for a group of



**Fig. 2.9** Electrical resistivity (a) and magnetic susceptibility (b) of superconducting  $\text{ReO}_{1-x}\text{FeAs}$  compounds with oxygen deficiency, as function of temperature [42]

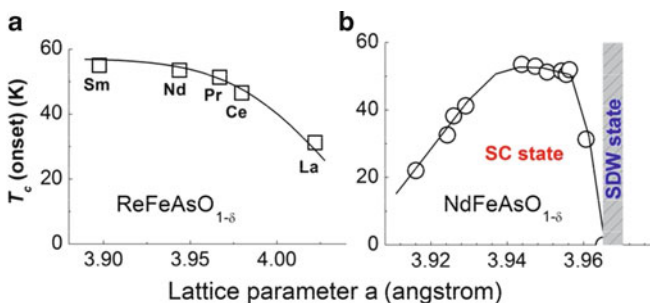
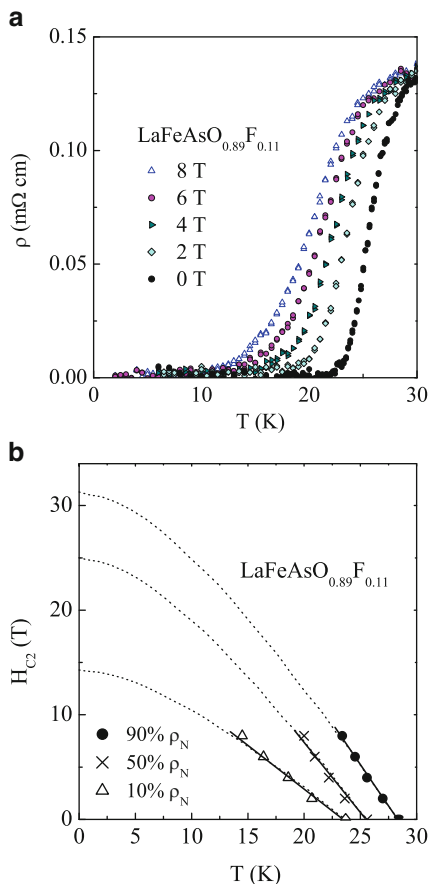


**Fig. 2.10**  $T_c$  in the row of  $\text{ReO}_{1-\delta}\text{FeAs}$  compounds as function of the lattice parameter  $a$  [42]

$\text{ReOFeAs}$  compounds with different rare-earth constituents are shown in Fig. 2.9 [42]. The behaviour of electrical conductivity and magnetic susceptibility in the vicinity of  $T_c$  is similar between different systems. We note that, differently from the  $\text{SmOFeAs}$  system of Fig. 2.8 which was doped with fluorine, all superconducting compounds collected in Fig. 2.9 are deficient in oxygen. Despite different nature of dopants – fluorine substitution or oxygen vacancies – the manifestation of superconducting state in the temperature dependence of electrical conductivity and magnetic susceptibility is identical for both systems. It is instructive to compare the superconducting transition temperatures throughout a row of compounds with different rare-earth elements and hence lattice parameter  $a$  (Fig. 2.10). We see that  $T_c$  decreases with the rise of  $a$  (due to the increase of the element’s ionic radius). For a given rare-earth constituent,  $T_c$  depends on the number of oxygen vacancies  $\delta$ . In a synthesized compound, the vacancy concentration is revealed by the lattice parameter  $a$  (Fig. 2.10b).

**Fig. 2.11** Temperature dependence of (a) electrical resistivity in different magnetic fields, and (b) the values of  $H_{c2}$  extracted from these data, for  $\text{LaO}_{0.89}\text{F}_{0.11}\text{FeAs}$  [23]



### 2.1.6 Critical Fields

Besides high transition temperatures, the FeAs-type compounds possess very high critical fields values. Consider, as an example, a study of the upper critical field  $H_{c2}$  in polycrystalline sample of  $\text{LaO}_{0.98}\text{F}_{0.11}\text{FeAs}$  with  $T_c = 28.2 \text{ K}$  [23].

$H_{c2}$  is estimated from the data on the temperature dependence of electrical resistivity in magnetic field. In Fig. 2.11a, such data in the field range up to 8 T are given, and in Fig. 2.11b, the  $H_{c2}(T)$  results extracted from the latter. It is seen from Fig. 2.11a that the interval of the drop in resistivity shifts towards lower temperatures on applying the field, that is typical for II order superconductors. The superconducting transition temperature  $T_c(H)$  is defined by the condition that  $\rho(T_c, H)$  equals a certain fraction (percentage) of resistivity  $\rho_N$  in the normal phase, for a given field magnitude  $H$ . The thus defined values of  $T_c(H)$  for  $\rho = 10, 30$  and 90% of  $\rho_N$  are shown in Fig. 2.11b along with the critical fields  $H_{c2}(T)$ . In all cases,  $H_{c2}(T)$  exhibit linear dependence without any tendency towards saturation.

The slope  $dH_{c2}/dT|_{T=T_c}$  equals  $-0.87$  T/K for  $\rho = 10\%\rho_N$ ,  $-1.41$  T/K for  $\rho = 50\%\rho_N$  and  $-1.59$  T/K for  $\rho = 90\%\rho_N$ . In the BCS theory, the  $H_{c2}$  is linear in  $T$  in the vicinity of  $T_c$  and saturates towards  $T = 0$ . According to the Werthamer–Helfand–Hohenberg formula [43],

$$H_{c2}(0) \approx -0.693 T_c \left. \frac{dH_{c2}}{dT} \right|_{T=T_c}. \quad (2.1)$$

The dashed lines in Fig. 2.11b are extrapolations of linear experimental curves towards the thus calculated values of  $H_{c2}(0)$ . For  $\rho = 90\%\rho_N$ , the  $H_{c2}(0)$  exceeds 30 T. From the known Ginsburg–Landau formula for the correlation length  $\xi(0) \approx (\Phi_0/2\pi H_{c2})^{1/2}$ , where  $\Phi_0$  is a flux quantum, an estimation follows:  $\xi(0) \approx 48$  Å for  $H_{c2}$  (10%  $\rho_N$ ),  $\xi(0) \approx 36$  Å for  $H_{c2}$  (50%  $\rho_N$ ),  $\xi(0) \approx 33$  Å for  $H_{c2}$  (90%  $\rho_N$ ). These values are comparable to those measured in cuprates for corresponding values of  $T_c$ .

Measurements of the Hall constant on the same sample revealed its negative sign (that corresponds to electron carriers) and carriers concentration of  $\approx 1.7 \cdot 10^{21}$  cm $^{-3}$  at room temperature and  $\approx 1 \cdot 10^{21}$  cm $^{-3}$  at a temperature just above  $T_c$  (assuming a single carriers band).

The above data concerning the sample studied of LaO $_{0.89}$ F $_{0.11}$ FeAs are quite representative for the whole series of superconducting compounds ReO $_{1-x}$ F $_x$ FeAs. Thus for NdO $_{0.82}$ F $_{0.18}$ FeAs with  $T_c = 51$  K [44],  $H_{c2}(48$  K) = 13 T has been measured, and the critical field  $H_{c2}(0)$  estimated after (2.1) turned out to be within 80–230 T. Measurements on a single crystal of the same composition [45] revealed a large anisotropy of  $H_{c2}$ .

The critical fields estimated after (2.1) for the field directions in the basal plane ( $ab$ ) and along the tetragonal axis ( $c$ ) are:  $H_{c2}^{ab}(0) \approx 304$  T and  $H_{c2}^c(0) \approx 62$ –70 T. The measurements on a Sm-based compound confirmed high values of  $H_{c2}$ . Thus for a sample SmO $_{0.85}$ F $_{0.15}$ FeAs with  $T_c = 46$  K, the measurements of specific heat in the fields of up to 20 T gave [46]  $[dH_{c2}/dT]_{T=T_c} = -5$  T/K, that according to (2.1) gives an estimate  $H_{c2}(0) = 150$  T. For another sample, SmO $_{0.7}$ F $_{0.3}$ FeAs [47] with  $T_c = 54.6$  K, the estimated  $H_{c2}(0)$  is even higher:  $H_{c2} \approx 200$  T. A detailed review of  $(H, T)$  phase diagrams of FeAs compounds can be found in [48].

### 2.1.7 Effect of Pressure on the $T_c$

Soon after the discovery of superconductivity in LaO $_{1-x}$ F $_x$ FeAs it was reported that in the compound with  $x = 0.11$ , the  $T_c$  increases under applied pressure and reaches the maximum value of 43 K at 4 GPa [49]. It was suggested that the lattice compression is responsible for this effect. Indeed, in ReOFeAs compounds the atoms of rare-earth element have smaller radius than La, and  $T_c$  in these compounds is markedly higher, exceeding 50 K. In a subsequent work [50], the measurements of electrical conductivity in LaOFeAs under high pressures, up to 29 GPa, have

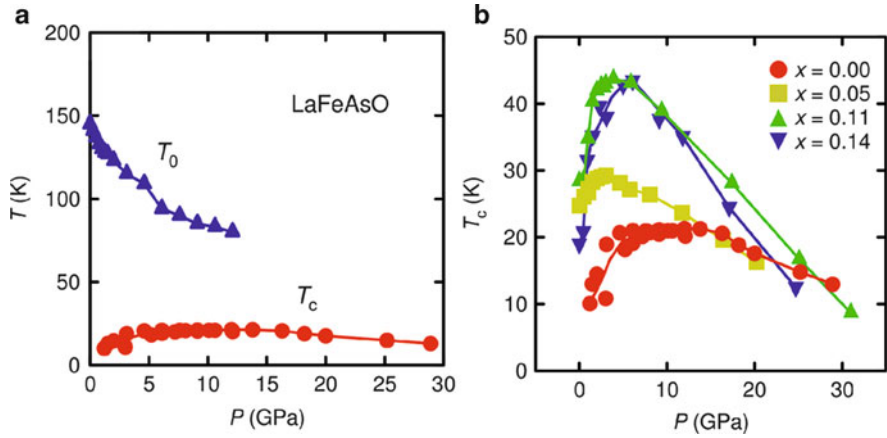


**Fig. 2.12** (a)  $(T, P)$  phase diagram for  $\text{LaOFeAs}$ , obtained from the measurements of electrical resistivity at different pressures [50]; (b) variation of  $T_c$  with pressure in  $\text{LaO}_{1-x}\text{F}_x\text{FeAs}$  compounds. The data for doped compounds are taken from [49, 51]

been done. The results concerning the variation of the temperatures of structural (magnetic) phase transition  $T_0$  and of the superconducting transition temperature, extracted from the raw data on  $\rho(T)$  at different pressures, are shown in Fig. 2.12.

The  $(P, T)$  phase diagram shown in Fig. 2.12a resembles the  $(x, T)$  phase diagram for doped  $\text{LaO}_{1-x}\text{F}_x\text{FeAs}$  compounds [8]. This similarity may be explained by an observation that the oxygen substitution with fluorine, beyond modifying the carriers density, results in reducing the lattice constant. Thus, as  $x = 0.05$  the unit cell squeezes from  $0.14186 \text{ nm}^3$  that is accompanied by an appearance of superconductivity with  $T_c = 24 \text{ K}$  [8]. According to the variation of the unit cell volume under pressure [51], the above variation corresponds to a pressure of  $\sim 0.3 \text{ GPa}$ . Correspondingly, in the context of merely changing the volume, the substitution of oxygen with fluorine is more efficient in suppressing structural and magnetic phase transitions and the onset of superconductivity than an effect of external pressure.

As is seen from Fig. 2.12b, the maximal  $T_c = 21 \text{ K}$  in stoichiometric compound  $\text{LaOFeAs}$  is achieved at the pressure of  $\sim 12 \text{ GPa}$ . As regards the variation of  $T_c$  with pressure in doped compounds, it first rises with pressure, passes through maximum and falls down. A similar behaviour of  $T_c$  under pressure is observed in  $\text{LaO}_{1-x}\text{F}_x\text{FeAs}$  of a different composition, as well as in oxygen-deficient  $\text{LaOFeAs}$  compounds (Fig. 2.13). The latter have maximal  $T_c \sim 50 \text{ K}$  at the pressure of  $1.5 \text{ GPa}$  [52].

A relation between the changes of  $T_c$  under pressure and variation of the lattice parameter is shown in Fig. 2.14. At high pressures ( $P > 10 \text{ GPa}$ ), the lattice parameters and  $T_c$  in the compound investigated  $\text{LaO}_{0.9}\text{F}_{0.1}\text{FeAs}$  do decrease linearly [53].

A similar behaviour of  $T_c$  under pressure was observed in another compound type,  $\text{LaOFeP}$ . At the ambient pressure,  $T_c$  in doped  $\text{LaO}_{1-x}\text{F}_x\text{FeP}$  compounds is

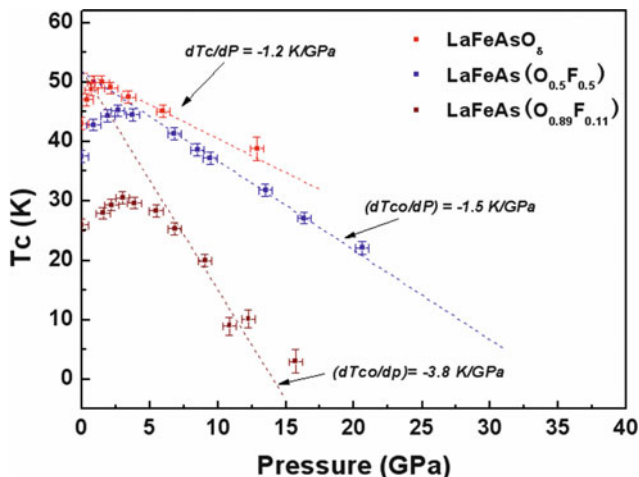


Fig. 2.13 Variation of the superconducting transition temperature with pressure for two  $\text{LaO}_{1-x}\text{F}_x\text{FeAs}$  compounds and a  $\text{LaO}_\delta\text{FeAs}$  compound with oxygen vacancies [52]

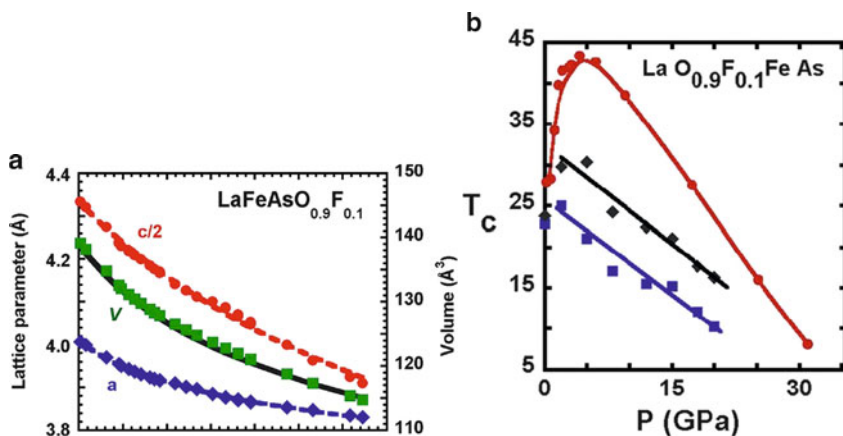
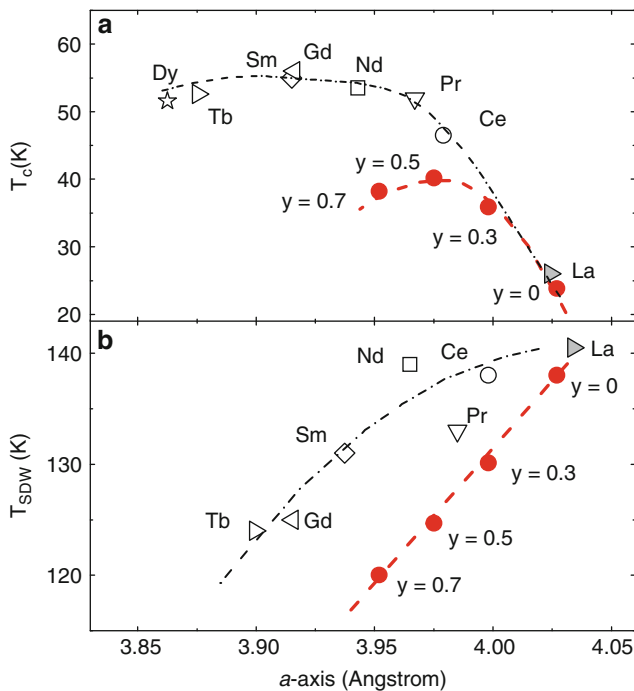


Fig. 2.14 Variation under pressure of (a) lattice parameters, and (b) superconducting transition temperature, for the  $\text{LaO}_{0.9}\text{F}_{0.1}\text{FeAs}$  compound [53]

2–7 K. On applying the pressure,  $T_c$  rises rapidly, achieving 8.8 K already at  $P = 0.8$  GPa, after which it falls down at the rate  $dT_c/dP > 4$  K/GPa [54].

Finally, we discuss an aspect of chemical pressure which occurs on a substitution of an ion in the compound by another ion of a smaller radius. In this case, the shrinking of the lattice parameter is observed as the dopant concentration grows. This situation is illustrated by Fig. 2.15, taken from [55].

Yttrium has smaller ionic radius than lanthanum, therefore replacing the latter by the former reduces the lattice parameter  $a$ . As is seen from the figure,  $T_c$  grows with the yttrium concentration, whereas  $T_N$  decreases. This trend is common for all



**Fig. 2.15** (a)  $T_c$  and (b)  $T_N$  for  $ReOFeAs$  compounds as functions of the lattice parameter. Black dots indicate the values of  $T_c$  and  $T_N$  for the  $La_{1-y}Y_yF_{0.15}FeAs$  compound at the levels of yttrium concentration  $y = 0; 0.3; 0.5; 0.7$  [55]

$ReO_{1-x}F_xFeAs$  compounds, which exhibit a maximum  $T_c$  value at some optimal fluorine doping  $x$ .

A doping of the stoichiometric compound  $LaOFeAs$  with yttrium up to  $y \leq 0.7$  does not lead to superconductivity, because an effect of chemical pressure is by far weaker than that of the fluorine doping. On yttrium doping of already superconducting compound  $LaO_{1-x}F_xFeAs$ ,  $T_c$  increases from 24 to 40 K. Obviously, this happens not so much due to a decrease of the lattice parameter (chemical pressure) as because of adding new carriers to the compound, as La is partially replaced by Y. Therefore, the role of chemical pressure at the onset of superconductivity in FeAs-based compounds is considerably limited, in comparison with the effect of doping by heterovalent elements.

A particularly interesting behaviour of superconductivity under pressure is observed in Ce-containing compounds. In general, compounds with Ce do often exhibit anomalies induced by the Kondo screening of localized moments of the  $4f$  shell of Ce atoms. In metallic Ce, an isostructural  $\alpha \rightarrow \Gamma$  phase transition under pressure occurs, whose nature is purely electronic one, induced by a change of the Ce valence [56].

In [57], based on a thorough study of transport properties and X-ray absorption spectra under pressure, a competition of superconductivity and Kondo screening was found in the  $\text{CeO}_{0.7}\text{F}_{0.3}\text{FeAs}$  compound. On increase of pressure, the superconducting transition temperature is gradually decreasing, and from  $P = 8.6$  GPa on it drops abruptly, reaching zero at  $P = 10$  GPa. XAS studies show a re-distribution of statistical weight from the main absorption line towards the satellite, indicating an appearance of the  $4f^0$  states in the main bulk of the  $4f^1$  states of Ce ions. A similar behaviour is observed in metallic Ce at the  $\alpha \rightarrow \Gamma$  transition, see [56].

Therefore, the X-ray absorption spectra reveal the Kondo screening of the localized moments at Ce ions, caused by pressure. The spectra of the superconducting state are similar to the XAS of pure Ce. Guided by this analogy, the authors of [57] arrived at a conclusion that the reason of the suppression of  $T_c$  by pressure in  $\text{CeO}_{0.7}\text{F}_{0.3}\text{FeAs}$  is in an emergence of a state with Kondo singlets, that expels the state with the Cooper pairs. Therefore, a quantum phase transition under pressure takes place, driven by a screening of localized moments of the  $\text{Ce}4f$  shell by the  $\text{Fe}3d$  electrons.

We mention in this relation the work [58], in which, in non-superconducting  $\text{CeOFeAs}_{1-x}\text{P}_x$ , two quantum critical points have been found, under the variation of the phosphorus content  $x$ . In the  $(T, x)$  phase diagram, for  $x < 0.37$  an antiferromagnetic phase was detected with an ordering of localized moments at Fe and Ce sites. Further on, in the  $0.92 < x < 1.00$  range a non-magnetic state with heavy fermions come about, induced by the Coulomb screening.

## 2.2 Magnetic Properties

### 2.2.1 Magnetic Structure

Stoichiometric  $\text{ReOFeAs}$  compounds are antiferromagnetics. The first indications of a possibility of magnetic ordering in  $\text{LaOFeAs}$  stem from measurements of temperature dependences of electrical conductivity and magnetic susceptibility, which exhibited anomalies near  $T \approx 150$  K. At this temperature, a structure transition from tetragonal into orthorhombic phase have been detected. It was initially suggested that the magnetic ordering occurs at the same temperature. By now, full neutron diffraction studies done at a nuclear reactor in Oak Ridge clarified the situation [59]. At  $T \approx 155$  K, indeed, a structural transition occurs with changing the symmetry from tetragonal space group  $P4/nmm$  to monoclinic  $P112/n$  at lower temperatures (in some cases a transition into orthorhombic phase  $Cmma$ ) has been detected).

It turned out that magnetic phase transition happens at a lower temperature,  $T_N = 137$  K. In neutron diffraction patterns, magnetic reflects (103), corresponding to doubling the primitive cell along the  $c$  axis, have been found. The main result of the study of  $\text{LaOFeAs}$  is shown in Fig. 2.16, where points and squares mark the